Interpretable Machine Learning Approaches for Assessing Maximum Force in Fiber-Reinforced Composites

Soheila Kookalani[1], Erika Parn[1], Ioannis Brilakis[2]

[1]Department of Engineering, University of Cambridge, Cambridge, UK.
[2]Laing O'Rourke Professor, Department of Engineering, University of Cambridge, Cambridge, UK.
sk2268@cam.ac.uk, eap47@cam.ac.uk, ib340@cam.ac.uk

Abstract

This paper investigates the accurate prediction of the maximum force in fiber-reinforced composites using the CatBoost machine learning algorithm. The study incorporates the Shapley additive explanations technique to enhance interpretability, revealing the significance of the impact of each variable on the output at both local and global scales. The research demonstrates that Shapley additive explanations provide valuable insights into the decision-making process of the machine learning model, identifying influential variables for specific instances and contributing to a comprehensive understanding of the overall model predictions. Notably, the alignment between the feature importance analyses from the machine learning model and Shapley additive explanations reinforces the significance of certain parameters in predicting maximum force as an interfacial property. The study advances the prediction of interfacial properties in fiber-reinforced composites and underscores the value of interpretable machine learning methods in offering insights into complex predictive models.

Keywords –

Machine learning; Interfacial properties; Maximum fore; Regression; Fiber-reinforced composites; Interpretability methods.

1 Introduction

Fiber-reinforced composites have become integral materials in civil engineering applications, owing to their remarkable combination of stiffness, strength, and lightweight properties [1]–[3]. The mechanical performance of these composites is primarily dictated by their interfacial properties [4], [5]. the determination of interfacial properties through fiber pullout tests involves labor-intensive and time-consuming experimental and numerical methods. Hence, there is a pressing need for an accurate and efficient alternative for predicting interfacial properties, essential for the design and customization of composite materials.

In recent years, machine learning (ML) techniques have emerged as promising substitutes for time-consuming simulation processes that offer the advantage of low computational cost and high accuracy [6]–[10]. For instance, Mangalathu and Jeon [11] employed lasso regression for beam-column joints. Yao et al. [12] demonstrated the superiority of two-class support vector regression (SVR) over one-class SVR and logistic regression in mapping landslide susceptibility. Chopra et al. [13] investigated the efficiency of ML models such as decision trees (DT), random forests (RF), and neural networks in estimating concrete compressive strength. Their findings revealed the superior efficiency of the neural network model, followed by the RF method. Additionally, Das et al. [14] introduced a data-driven physics-informed approach for concrete crack estimation, showcasing the capability to predict infrastructure service life based on real-time monitoring data.

In this study, the CatBoost algorithm is employed to predict the maximum force in fiber-reinforced composites. A grid search approach and K-fold cross-validation are employed, utilizing a dataset comprising 922 samples to identify the optimum parameters of the ML model. Understanding why an ML model produces specific estimations and identifying the features influencing those estimations is crucial. Therefore, the Shapley additive explanations (SHAP) method is applied to comprehend the behavior of the ML model. The paper is organized as follows: Section 2 introduces SHAP as an interpretable ML approach; Section 3 presents a numerical example for maximum force prediction, and finally, Section 4 offers concluding remarks and future directions.

2 Interpretable ML approach

In addressing the inherent black-box nature of ML models, particularly in the context of predicting the maximum force in fiber-reinforced composites, this study employs an interpretable ML approach. The opaqueness of such black-box models can lead to a diminished level of trust and understanding, impeding their broader acceptance and applicability.

In this study, the SHAP approach is employed for model interpretation to mitigate this challenge. The SHAP technique draws inspiration from conditional expectation and game theory [15]. It provides a systematic framework for assessing the impact of individual input features on the predictions of the model, thereby offering a clearer understanding of the decision-making process.

The central idea behind SHAP lies in evaluating the significance of each feature by assessing the increase in estimation error after modifying the values of a given factor. A feature is deemed significant if its manipulation results in a substantial increase in prediction error; conversely, a feature is considered non-significant if its alteration has little impact on the error. This approach allows us to identify and prioritize the input features that contribute most significantly to the predictions of the model, thereby enhancing interpretability.

In essence, SHAP aids in ranking the features based on their contribution to the decision-making process, highlighting the interactions and relationships among these features. The interpretability framework is constructed on the principles of additive feature attribution, wherein the output model is represented as a linear function comprising the sum of the actual values associated with each parameter.

The interpretable framework developed through SHAP provides a transparent and comprehensible representation of the decision logic of the ML model. This approach not only enhances the trustworthiness of predictions by elucidating the role and influence of individual features but also contributes to the broader adoption of ML techniques in assessing the maximum force in fiber-reinforced composites. The resulting interpretable model serves as a valuable tool for practitioners and researchers seeking to bridge the gap between advanced ML capabilities and a clear understanding of the underlying mechanics in composite material.

3 Numerical examples

The assessment of F_{max} in fiber-reinforced composites can be effectively carried out using dependable quantitative methods such as the fiber pullout test and simulation. In this study, a thorough compilation of 922 fiber pullout outcomes from existing literature forms a comprehensive dataset [16]–[27].

The input data comprises 11 distinct features, providing details on fiber characteristics, sample preparation environment, and testing conditions. The resulting output, F_{max}, represents an interfacial property. Table 1 outlines the specified ranges for these parameters.

Table 1. Statistical attributes of dataset.

Attribute	Unit	Minimum	Maximum
Type of fiber	-	1	10
Fiber diameter	μm	5	300
Embedded length	μm	24.5	2018
Young’s modulus of fiber	GPa	3.39	294
Poisson’s ratio of fiber	-	0.17	0.37
Type of matrix	-	1	10
Young’s modulus of matrix	GPa	1.2	3.96
Poisson’s ratio of matrix	-	0.31	0.37
Loading rate	m/s	0.0017	6
Prepare temperature	℃	20	370
Test temperature	℃	-196	120
F_{max}	N	0.005	1.902

Figure 1 illustrates the correlation matrix of the input parameters, where each correlation coefficient signifies the degree of interaction between two parameters. In this paper, any correlation exceeding 0.70 is considered a significant dependency. The matrix reveals a significant association, with a correlation of 0.95, between embedded length and fiber diameter. Additionally, there is a correlation coefficient of 0.79 between embedded length and fiber type. Moreover, the correlation coefficient between the type of fiber and fiber diameter stands at 0.73. Notably, there are no evident correlations observed for the remaining parameters.

Figure 1. Correlation matrix for input variables

3.1 Regression model

In this paper, a comparative study has been conducted to determine the best regression model. The investigation encompasses several regression algorithms, namely decision tree (DT), AdaBoost, and CatBoost. Through rigorous analysis and comparison, the aim is to identify the most suitable regression model for the given dataset.

The process of fine-tuning the hyperparameters for ML models involves utilizing a grid search approach combined with 10-fold cross-validation to prevent overfitting. Consequently, the hyperparameter values that yield the best performance are chosen for the ML approaches. The optimal hyperparameter values for the regression algorithms are presented in Table 2. The average R^2 and RMSE values resulting from 10-fold cross-validation are presented in Table 3.

Table 2. Optimal hyper parameters.

Model	Optimal configuration
DT	Max_depth=6, min_samples_leaf=1, min_samples_split=2, random_state=3
AdaBoost	Learning_rate=1, n_estimators=50, random_state=0
CatBoost	Depth=8, iterations=1000, learning_rate=0.01

Table 3. Performance of regression models.

Model	Average R^2	Average RMSE
DT	0.988	0.028
AdaBoost	0.982	0.039
CatBoost	0.997	0.018

As a result of the comparative study, the CatBoost model exhibits the highest accuracy. Figure 2 displays the regression plot of the CatBoost model, confirming its high accuracy. The x-axis illustrates the actual data, whereas the y-axis denotes the predicted data. The plot illustrates the correlation between actual and predicted values. A notable observation is that a significant portion of the data points closely align with the regression line, indicating a strong predictive accuracy. In the subsequent subsection, the CatBoost model is further explored as an interpretable method.

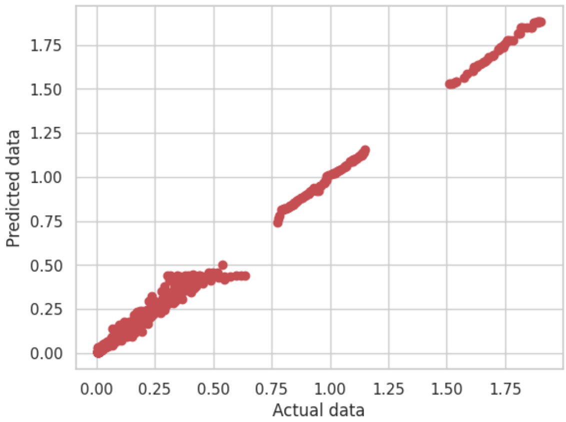

Figure 2. Regression plot

3.2 Interpretable method

Illustrated in Figure 3 is the significance of parameters in shaping the CatBoost model, taking into account their contributions to each tree. The most influential feature is the fiber diameter, followed by the embedded length. Conversely, the loading rate holds the least importance, with the Poisson's ratio of the matrix following as the next less critical variable. Notably, discerning whether an input variable exerts positive or negative effects on the relative importance plots is unfeasible.

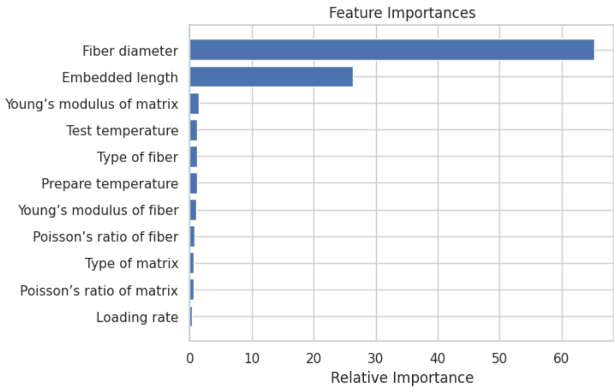

Figure 3. CatBoost importance factor

Figure 4a illustrates the SHAP summary plot, where individual points correspond to Shapely values for the parameters. Each row in the plot contains an equal number of samples. The Shapely values and input variables are represented on the *x*-axis and *y*-axis, respectively. The variables are arranged in descending order of importance, with the most crucial variable positioned at the top. Samples with the same SHAP value for a factor are dispersed along the horizontal axes. High variable values are depicted in red, while low values are in blue. The red color signifies the range of values that elevate the SHAP value and, consequently, the associated estimation.

Observations indicate that an increase in the Young's modulus of the fiber, preparation temperature, and Poisson's ratio of the matrix results in a reduction of the SHAP value, leading to a decrease in F_{max}. Conversely, an increase in embedded length, fiber diameter, and Poisson's ratio of the fiber contributes to an elevation in the F_{max} value. Figure 4a maintains an equal distribution of points in each row.

In Figure 4b, the global significance factor is presented as the mean of the absolute SHAP value per factor. According to SHAP analysis, the input parameters of embedded length and fiber diameter are identified as the most crucial, aligning with findings from the CatBoost significance variable.

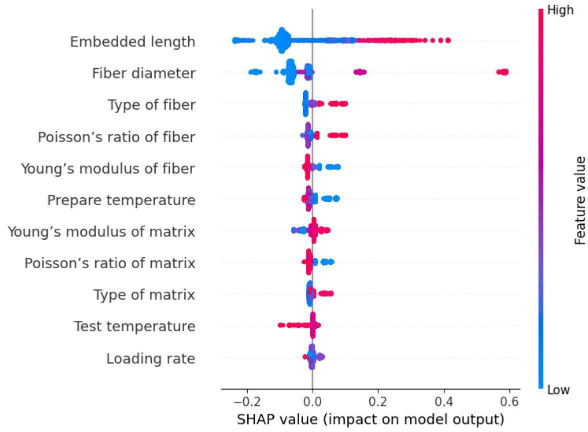

(a)

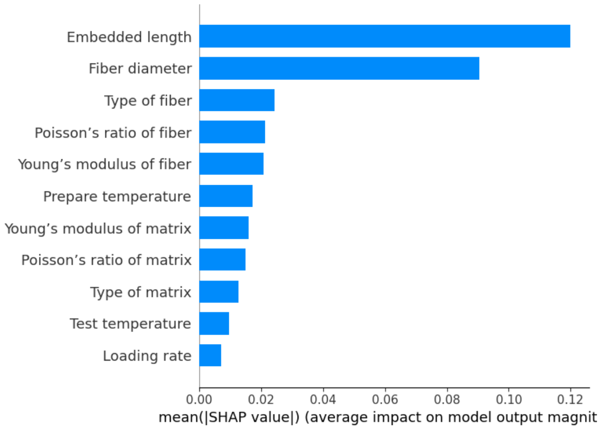

(b)

Figure 4. SHAP plots: (a) Shapely value; (b) Global importance factor.

Figure 5 illustrates the presentation of the SHAP dependence graph, which takes the form of a scatter plot depicting the SHAP value of a parameter in relation to other parameters. The color representation in the figure indicates the impact of interactions with other variables on the horizontal axis values. Notably, a majority of these interactions exhibit non-linear behavior. In Figure 5a, the influence of the type of fiber on embedded length is showcased, revealing that, except for the type of fiber equal to 10, the SHAP value tends to decrease with an increase in embedded length. Additionally, positive effects are predominantly noticeable in the case of fiber diameter and the Poisson's ratio of the fiber, as depicted in Figure 5b. Figure 5g highlights that the Young's modulus of the matrix has a predominantly negative impact on the SHAP value concerning the input parameter of embedded length. The remaining plots indicate that the negative effect is generally more pronounced for the other variables.

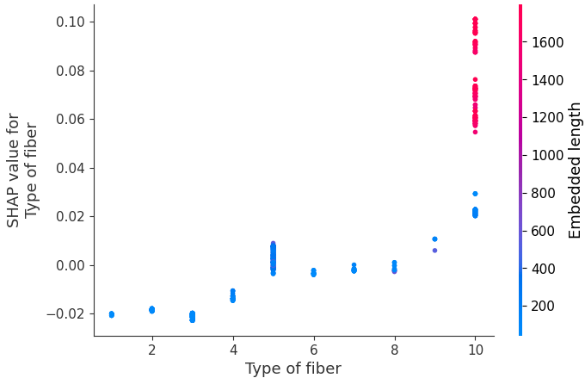

(a)

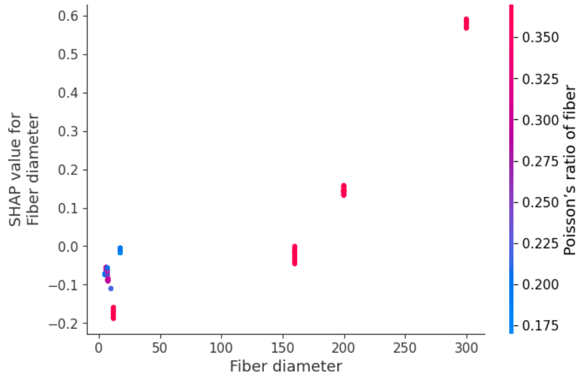

(b)

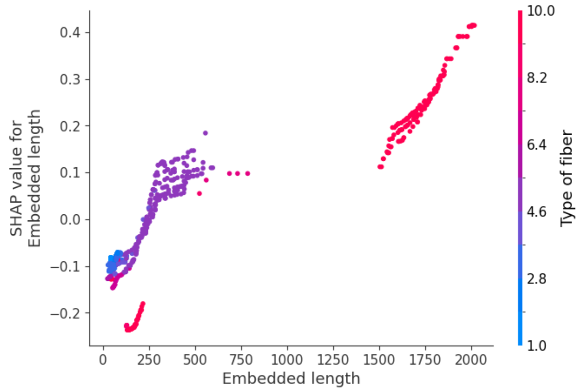

(c)

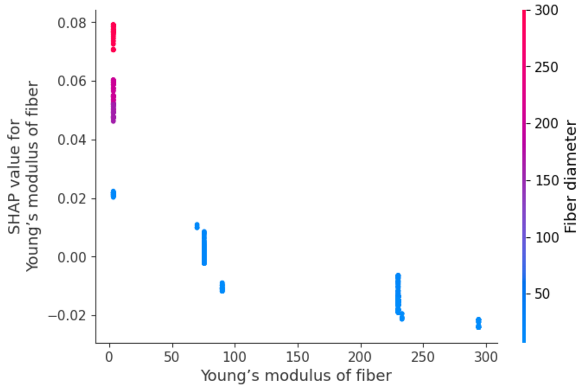

(d)

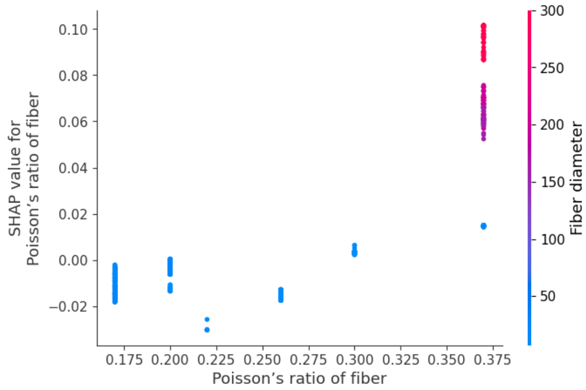

(e)

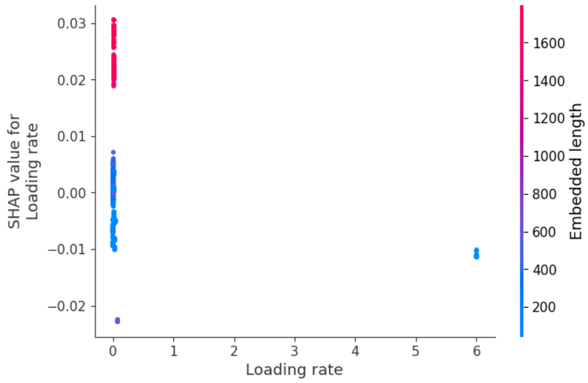

(i)

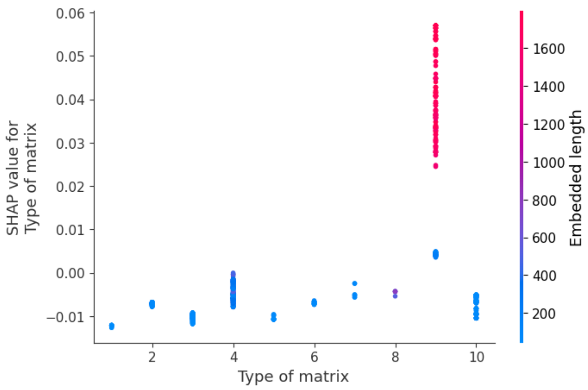

(f)

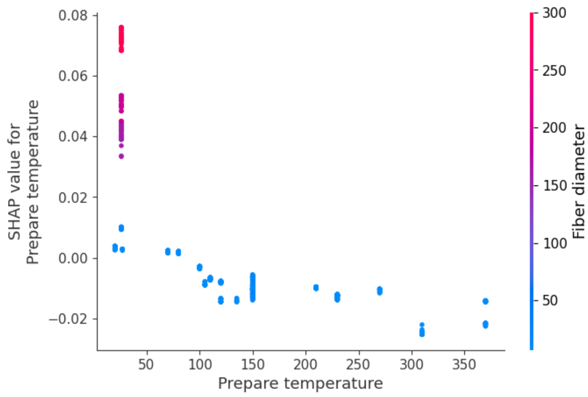

(j)

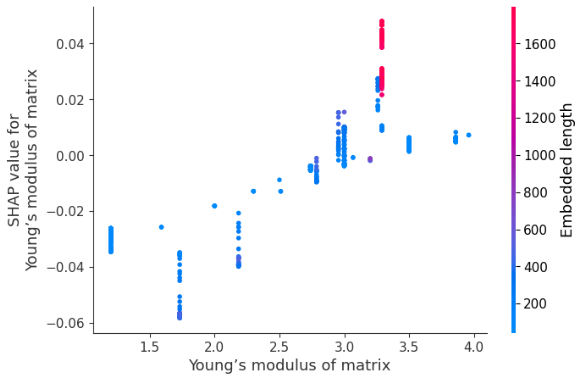

(g)

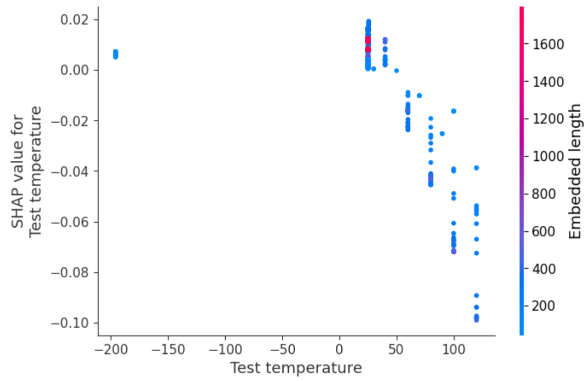

(k)

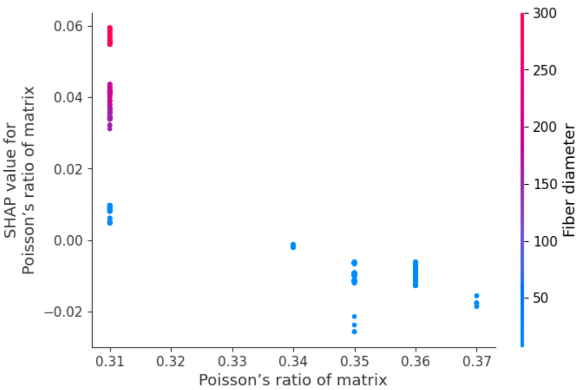

(h)

Figure 5. SHAP partial dependence plots.

4 Conclusions

This study presents an exploration of interpretable ML approaches for predicting the maximum force in fiber-reinforced composites during pullout tests. The investigation focuses on the CatBoost algorithm, utilizing a dataset of 922 samples with 11 features as inputs to the ML model. The performance of the CatBoost model is found to be exceptional, exhibiting high accuracy with R^2 values of 0.997 and RMSE values of 0.018.

The CatBoost algorithm is coupled with the SHAP interpretable approach to enhance the transparency and interpretability of the ML model. This step is crucial for elucidating the predictions made by the ML model, providing insights into the relative importance of input features. SHAP, chosen for its comprehensive explanatory capabilities, proves to be a valuable tool in understanding the trends and contributions of individual parameters. Remarkably, the SHAP values highlight embedded length and fiber diameter as the most influential variables, positively impacting the estimation of the maximum force.

Furthermore, the congruence between the features identified as significant by both the CatBoost method and SHAP underscores the reliability and consistency of the proposed approach. This alignment strengthens confidence in the interpretability of the ML model and the robustness of the identified influential parameters.

While this study focuses on fiber-reinforced composites, the methodology developed herein holds promise for broader applications in structural performance estimation across diverse systems. The successful implementation of the proposed approach creates opportunities for future research, which will extend the methodology to predict other interfacial properties of fiber-reinforced composites. This expansion not only contributes to the versatility of the developed methodology but also underscores its potential impact on advancing the understanding and prediction of structural behavior in various engineering applications.

Acknowledgment

The financial support of EPSRC via grant number EP/W018705/1 is gratefully acknowledged.

References

[1] K. M. Liew, Z. X. Lei, and L. W. Zhang, "Mechanical analysis of functionally graded carbon nanotube reinforced composites: A review," *Compos Struct*, vol. 120, pp. 90–97, Feb. 2015, doi: 10.1016/J.COMPSTRUCT.2014.09.041.

[2] K. M. Liew, Z. Z. Pan, and L. W. Zhang, "An overview of layerwise theories for composite laminates and structures: Development, numerical implementation and application," *Compos Struct*, vol. 216, pp. 240–259, May 2019, doi: 10.1016/J.COMPSTRUCT.2019.02.074.

[3] K. M. Liew, Z. Pan, and L.-W. Zhang, "The recent progress of functionally graded CNT reinforced composites and structures," *Sci. China-Phys. Mech. Astron*, vol. 63, no. 3, p. 234601, 2020, doi: 10.1007/s11433-019-1457-2.

[4] E. B. Callaway, P. G. Christodoulou, and F. W. Zok, "Deformation, rupture and sliding of fiber coatings in ceramic composites," *J Mech Phys Solids*, vol. 132, p. 103673, Nov. 2019, doi: 10.1016/J.JMPS.2019.07.016.

[5] W. H. Liu, L. W. Zhang, and K. M. Liew, "Modeling of crack bridging and failure in heterogeneous composite materials: A damage-plastic multiphase model," *J Mech Phys Solids*, vol. 143, p. 104072, Oct. 2020, doi: 10.1016/J.JMPS.2020.104072.

[6] S. Kookalani and B. Cheng, "Structural Analysis of GFRP Elastic Gridshell Structures by Particle Swarm Optimization and Least Square Support Vector Machine Algorithms," *Journal of Civil Engineering and Materials Application*, vol. 5, no. 3, pp. 139–150, Sep. 2021, doi: 10.22034/JCEMA.2021.304981.1064.

[7] S. Kookalani and B. Cheng, "Structural Analysis of GFRP Elastic Gridshell Structures by Particle Swarm Optimization and Least Square Support Vector Machine Algorithms," *Journal of Civil Engineering and Materials Application is published by Pendar Pub*, vol. 5, no. 3, pp. 139–150, 2021, doi: 10.22034/jcema.2021.304981.1064.

[8] S. Kookalani, B. Cheng, and S. Xiang, "Shape optimization of GFRP elastic gridshells by the weighted Lagrange ε-twin support vector machine and multi-objective particle swarm optimization algorithm considering structural weight," *Structures*, vol. 33, pp. 2066–2084, 2021, doi: 10.1016/j.istruc.2021.05.077.

[9] S. Kookalani, S. Nyunn, and S. Xiang, "Form-finding of lifting self-forming GFRP elastic gridshells based on machine learning interpretability methods," *STRUCTURAL ENGINEERING AND MECHANICS*, vol. 84, no. 5, pp. 605–618, 2022.

[10] S. Kookalani, B. Cheng, and J. L. C. Torres, "Structural performance assessment of GFRP elastic gridshells by machine learning interpretability methods," *Frontiers of Structural and Civil Engineering*, vol. 16, no. 10, pp. 1249–1266, 2022, doi: 10.1007/s11709-022-0858-5.

[11] S. Mangalathu and J. S. Jeon, "Classification of failure mode and prediction of shear strength for reinforced concrete beam-column joints using machine learning techniques," *Eng Struct*, vol. 160, pp. 85–94, 2018, doi: 10.1016/j.engstruct.2018.01.008.

[12] X. Yao, L. G. Tham, and F. C. Dai, "Landslide susceptibility mapping based on Support Vector

Machine: A case study on natural slopes of Hong Kong, China," *Geomorphology*, vol. 101, no. 4, pp. 572–582, 2008, doi: 10.1016/j.geomorph.2008.02.011.

[13] P. Chopra, R. K. Sharma, M. Kumar, and T. Chopra, "Comparison of Machine Learning Techniques for the Prediction of Compressive Strength of Concrete," *Advances in Civil Engineering*, 2018, doi: 10.1155/2018/5481705.

[14] S. Das, S. Dutta, C. Putcha, S. Majumdar, and D. Adak, "A Data-Driven Physics-Informed Method for Prognosis of Infrastructure Systems: Theory and Application to Crack Prediction," *ASCE ASME J Risk Uncertain Eng Syst A Civ Eng*, vol. 6, no. 2, p. 04020013, 2020, doi: 10.1061/ajrua6.0001053.

[15] S. M. Lundberg and S. I. Lee, "A unified approach to interpreting model predictions," *Adv Neural Inf Process Syst*, vol. 30, 2017.

[16] L. Wenbo *et al.*, "Interfacial shear strength in carbon fiber-reinforced poly(phthalazinone ether ketone) composites," *Polym Compos*, vol. 34, no. 11, pp. 1921–1926, Nov. 2013, doi: 10.1002/PC.22599.

[17] C. Zhi, H. Long, and M. Miao, "Microbond testing and finite element simulation of fibre-microballoon-epoxy ternary composites," *Polym Test*, vol. 65, pp. 450–458, Feb. 2018, doi: 10.1016/J.POLYMERTESTING.2017.12.029.

[18] B. Liu, Z. Liu, X. Wang, G. Zhang, S. Long, and J. Yang, "Interfacial shear strength of carbon fiber reinforced polyphenylene sulfide measured by the microbond test," *Polym Test*, vol. 32, no. 4, pp. 724–730, Jun. 2013, doi: 10.1016/J.POLYMERTESTING.2013.03.020.

[19] Q. Li, G. Nian, W. Tao, and S. Qu, "Size effect on microbond testing interfacial shear strength of fiber-reinforced composites," *Journal of Applied Mechanics, Transactions ASME*, vol. 86, no. 7, Jul. 2019, doi: 10.1115/1.4043354/726015.

[20] M. Sato, J. Koyanagi, X. Lu, Y. Kubota, Y. Ishida, and T. E. Tay, "Temperature dependence of interfacial strength of carbon-fiber-reinforced temperature-resistant polymer composites," *Compos Struct*, vol. 202, pp. 283–289, Oct. 2018, doi: 10.1016/J.COMPSTRUCT.2018.01.079.

[21] Q. Li, G. Nian, W. Tao, and S. Qu, "Temperature-Dependent Interfacial Debonding and Frictional Behavior of Fiber-Reinforced Polymer Composites," *Journal of Applied Mechanics, Transactions ASME*, vol. 86, no. 9, Sep. 2019, doi: 10.1115/1.4044017/955633.

[22] M. Yan *et al.*, "Simulation and measurement of cryogenic-interfacial-properties of T700/modified epoxy for composite cryotanks," *Mater Des*, vol. 182, p. 108050, Nov. 2019, doi: 10.1016/J.MATDES.2019.108050.

[23] R. Dsouza *et al.*, "3D interfacial debonding during microbond testing: Advantages of local strain recording," *Compos Sci Technol*, vol. 195, p. 108163, Jul. 2020, doi: 10.1016/J.COMPSCITECH.2020.108163.

[24] M. Nishikawa, T. Okabe, K. Hemmi, and N. Takeda, "Micromechanical modeling of the microbond test to quantify the interfacial properties of fiber-reinforced composites," *Int J Solids Struct*, vol. 45, no. 14–15, pp. 4098–4113, Jul. 2008, doi: 10.1016/J.IJSOLSTR.2008.02.021.

[25] N. S. Choi and J. E. Park, "Fiber/matrix interfacial shear strength measured by a quasi-disk microbond specimen," *Compos Sci Technol*, vol. 69, no. 10, pp. 1615–1622, Aug. 2009, doi: 10.1016/J.COMPSCITECH.2009.03.012.

[26] H. Wang, X. Zhang, Y. Duan, and L. Meng, "Experimental and Numerical Study of the Interfacial Shear Strength in Carbon Fiber/Epoxy Resin Composite under Thermal Loads," *Int J Polym Sci*, vol. 2018, 2018, doi: 10.1155/2018/3206817.

[27] X. Wang *et al.*, "Effects of thermal residual stress on interfacial properties of polyphenylene sulphide/carbon fibre (PPS/CF) composite by microbond test," *J Mater Sci*, vol. 51, no. 1, pp. 334–343, Jan. 2016, doi: 10.1007/S10853-015-9251-2/TABLES/2.